CURVATURE DUCTILITYOF REINFORCED CONCRETE COLUMN SECTIONS UNDER DIFFERENT STRAIN RATES

Dr. Thamir K. Al-Azawi **Professor**

Dr. Raad K. Al Azawi **Lecturer**

Teghreed H. Ibrahim

Civil Eng. Dept.
College of Eng.- University of Baghdad.

ABSTRACT

This paper presents theoretical parametric study of the curvature ductility capacity for reinforced concrete column sections. The study considers the behavior of concrete and reinforcing steel under different strain rates. A computer program has been written to compute the curvature ductility taking into account the spalling in concrete cover. Strain rate sensitive constitutive models of steel and concrete were used for predicting the moment-curvature relationship of reinforced concrete columns at different rate of straining. The study parameters are the yield strength of main reinforcement, yield strength of transverse reinforcement, compressive strength of concrete, spacing of ties and the axial load. The results indicated that higher strain rates improve both the curvature ductility and the moment capacity of reinforced concrete column sections.

KEYWORDS

Curvature Ductility, Columns, Reinforced Concrete, Strain Rate.

NOTATIONS

f_c' = concrete cylinder strength**.**

f_{cc}',f_{co}'= confined & unconfined concrete compressive strength in members.

f_y =steel yield strength.

f_y' =dynamic yield strength of steel.

f_u =static ultimate yield strength of steel.

f_u' =dynamic ultimate yield strength of steel.

f_{yt} =yield strength of transverse reinforcement.

f_{Le}' = equivalent uniform lateral pressure.

f_L = average confinement pressure.

ε_c =concrete strain.

ε_1 =strain corresponding to peak stress of confined concrete.

ε_{01} =strain corresponding to peak stress of unconfined concrete.

ε_{85} =strain corresponding to 85% of peak stress of confined concrete.

ε_{085} =strain corresponding to 85% of peak stress of unconfined concrete on the descending branch.

ε_h =static strain hardening initiation strains of steel.

ε_h' =dynamic strain hardening initiation strains of steel.

ε_u =static ultimate strains of steel.

ε_u' =dynamic ultimate strains of steel.

$\acute{\varepsilon}$ =strain rate $\geq 10^{-5}$

E_c =modulus of elasticity for concrete.

E_{sec} =secant modulus of elasticity for concrete.

E_s =modulus of elasticity for steel.

ρ_c =total transverse steel area in two orthogonal directions divided by corresponding concrete area.

A_{sx}, A_{sy}=area of one leg of transverse reinforcement in x and y directions.

b_{cx}, b_{cy}=core dimensions measured c/c of perimeter hoop in x and y directions.

m, n =number of tie legs in x and y directions.

S =spacing of transverse reinforcement.

S_L =spacing of longitudinal reinforcement laterally supported by corner of hoop or hook of cross tie.

INTRODUCTION

Usually it is desirable to design a reinforced concrete member with sufficient curvature ductility capacity to avoid brittle failure in flexure and to insure a ductile behavior, especially under seismic conditions. The philosophy of seismic design for moment resisting reinforced concrete frames is based on the formation of plastic hinges at the critical sections of the frame under the effect of substantial load reversals in the inelastic range. The ability of the plastic hinge to undergo several cycles of inelastic

deformation without significant loss in its strength capacity is usually assessed in terms of the available ductility of the particular reinforced concrete section.

The ductility capacity of reinforced concrete sections is usually expressed in terms of the curvature ductility ratio ($\mu_{ø}=ø_u/ø_y$) where $ø_y$ is the curvature of the section at first yield of the tensile reinforcement and $ø_u$ is the maximum curvature corresponding to a specific ultimate concrete compression strain.

The moment-curvature analysis of the section is usually performed under monotonically increasing load which represents the first quarter-cycle of the actual hysteretic behavior of the plastic hinge rotation under the earthquake loading. Therefore, $\mu_{ø}$ of a section calculated under such assumption is a theoretical estimate of the actual inherent ductility of the section when subjected to an actual earthquake loading. However, the theoretical estimation of $\mu_{ø}$ under monotonic loading is widely used as an appropriate indicator of the adequacy of earthquake resistant design for reinforced concrete members.

Soroushian and Sim (1986) [1] used strain rate sensitive constitutive models for steel and concrete to predict the axial load-axial strain relationship of reinforced concrete rectangular columns at different rates of strain. The analysis parameters were the yield strength of reinforcement (f_y =276, 414, 552 MPa), the concrete strength (f_c'=20.7, 27.6 MPa), the steel ratio (ρ=0.026, 0.032, 0.04) and the amounts of hoop reinforcement (ρ_s=0.01388,

0.02082, 0.04164). The results indicated that for the range of analysis parameters considered and for the range of strain rates of (0.00005/sec - 0.5/sec) the secant axial stiffness increases in the range of (16%-36%). Al-Haddad (1995) [2] studied the curvature ductility for reinforced concrete beams under strain rates in a range of (static, 0.05 and 0.1/sec) for values of (f_y =414, 440, 483, 518 MPa) and reinforcement ratio (ρ=0.003, 0.3). He assumed that only the steel reinforcement is a strain rate sensitive. The results indicated that for a strain rate of (0.05/sec) the curvature ductility ratio was decreased by about (12%) for an increase of (34.5 MPa) in f_y compared with that under static loading.

MATERIAL MODELS OF THE PRESENT STUDY

Constitutive Concrete Model

The concrete constitutive model adopted in the present study is that of Razvi & Saatcioglu (1999) [3] which takes into account the cross sectional shape and reinforcement arrangements, Fig.(1). The effect of the strain rate had been accounted for in this model by using the two coefficients (k_f, k_ε) as had been derived by Soroushian (1986) [1] on the test results basis.

The ascending part of the proposed curve is represented by:

$$f_c = \frac{f_{cc}'.k_f.(\frac{\varepsilon_c}{\varepsilon_1.k_\varepsilon}).r}{r-1+(\frac{\varepsilon_c}{\varepsilon_1.k_\varepsilon})^r} \qquad \ldots\ldots\ldots\ldots\ldots\ldots\ldots\ldots\ldots\ldots(1)$$

Where:

$$r = \frac{E_c}{E_c - E_{\sec}} \quad , \quad E_{\sec} = \frac{f_{cc'}.k_f}{\varepsilon_1.k_\varepsilon} \quad , \quad E_c = 4730\sqrt{f_{c'}}$$

Where f_c' in MPa.

All the parameters are as defined in the notations list.

The descending part assumes a slope that changes with confinement reinforcement and as follows:-

$$\varepsilon_1 = \varepsilon_{01}(1+5k_3K)$$

$$\varepsilon_{85} = 260k_3.\rho_c.\varepsilon_1[1+0.5k_2(k_4-1)]+\varepsilon_{085} \qquad \cdots\cdots\cdots\cdots\cdots\cdots(2)$$

$$k_3 = \frac{40}{f_{c'o}} \le 1 \quad , \quad k_1 = 6.7(f_{le})^{-0.17}$$

$$k_4 = \frac{f_{Le}}{500} > 1 \quad , \quad K = \frac{k_1.f_{Le}}{f_{c'o}}$$

$$k_2 = 0.15\sqrt{\left(\frac{b_c}{S}\right)\left(\frac{b_c}{SL}\right)} \le 1$$

$$\varepsilon_{01} = 0.0028 - 0.008k_3$$

$$\varepsilon_{085} = \varepsilon_{01} + 0.0018k_3^2$$

$$\rho_c = \frac{\sum_{i=1}^{n}(A_{sx})_i + \sum_{j=1}^{m}(A_{sy})_j}{S(b_{cx}+b_{cy})}$$

$$f_{Le} = k_2 f_L$$

$$k_f = 1.48 + 0.16\log_{10}\varepsilon^{\bullet} + 0.0127(\log_{10}\varepsilon^{\bullet})^2$$

$$k_\varepsilon = 1.08 + 0.112\log_{10}\varepsilon^{\bullet} + 0.0193(\log_{10}\varepsilon^{\bullet})^2$$

Figure (2) shows the constitutive model of concrete adopted in the present study for two different strain rates as compared with the experimental results of Soroushian and Sim [1]

also with the models of modified Kent and Park [4] and Soroushian [1].

Constitutive Steel Model

Several models were proposed to represent the stress-strain relationship of steel reinforcement by using many dynamic tests results. The following constitutive model of steel has been empirically derived by Parvis Soroushian (1987) [5] from dynamic test results on structural steel, reinforcing bars and deformed wires for different wires and for different types of steel.

$$f_s = \begin{cases} E_s\varepsilon_s \cdots\cdots\cdots\cdots\cdots\cdots\cdots\cdots\cdots\cdots\cdots\cdots if \quad \varepsilon_s < \dfrac{f_y'}{E_s} \\ f_y' \cdots\cdots\cdots\cdots\cdots\cdots\cdots\cdots\cdots\cdots\cdots\cdots if \quad \dfrac{f_y'}{E_s} < \varepsilon_s < \varepsilon_h' \\ f_y'\left[\dfrac{112(\varepsilon_s-\varepsilon_h')+2}{60(\varepsilon_s-\varepsilon_h')+2}+\dfrac{(\varepsilon_s-\varepsilon_h')}{(\varepsilon_u'-\varepsilon_h')}\left(\dfrac{f_u'}{f_y'}-1.7\right)\right] if \quad \varepsilon_h' < \varepsilon_s < \varepsilon_u' \\ 0.0 \cdots\cdots\cdots\cdots\cdots\cdots\cdots\cdots\cdots\cdots\cdots\cdots if \quad \varepsilon_s \geq \varepsilon_u' \end{cases} \cdots(3)$$

Where:

$$f_y' = f_y[(-6.54*10^{-8} f_y + 1.46) + (-1.334*10^{-7} f_y + 0.0927)\log_{10}\varepsilon^{\cdot}] \cdots\cdots(4)$$

$$f_u' = f_u[(-1.118*10^{-7} f_y + 1.15) + (-0.354*10^{-7} f_y + 0.04969)\log_{10}\varepsilon^{\cdot}] \cdots(5)$$

$$\varepsilon_h' = \varepsilon_h[(-6.105*10^{-6} f_y + 4.46) + (-1.22*10^{-6} f_y + 0.693)\log_{10}\varepsilon^{\cdot}] \cdots\cdots(6)$$

$$\varepsilon_u' = \varepsilon_u[(-1.295*10^{-6} f_y + 1.4) + (-2.596*10^{-7} f_y + 0.0827)\log_{10}\varepsilon^{\cdot}] \cdots(7)$$

Figure (3) shows the comparison between the experimental (f-ε) curve and Parvis Soroushian (1987) [5] constitutive model for two different strain rates for steel specimens with yield strength of (235 MPa). Based on equations (3-7), table (1) gives

the dynamic to static ratios of the yield and ultimate stresses of steel and its strain hardening and ultimate stresses of steel and its strain hardening and ultimate strains for (f_y=307, 345, 414 MPa) and for a range of strain rates of (10^{-5}-1)/sec.

Moment-Curvature Relationship for Concrete Sections

The response of reinforced concrete cross section to an applied bending moment and an axial force may be adequately described by the relation between moment and curvature referred to moment-curvature relationship. This relation depends on the material and geometrical properties of cross section as well as the level of the applied axial force.

This relationship is established using the following procedure:

1. The ultimate concrete compressive strain is first computed using Bing, Park and Tanka (2001)[6] equation and as follows:

$$\varepsilon_{cu} = \varepsilon_{co}[2 + (122.5 - 0.92 f_{co})\sqrt{\frac{f_l}{f_{co}}}] \quad \cdots\cdots\cdots\cdots\cdots \quad (8)$$

Where:

f_l =lateral confining stress of transverse reinforcing steel

f_{co} =compressive strength of unconfined concrete

ε_{co}=strain at peak stress of unconfined concrete

The concrete spalling strain is limited by (0.004) as reported in Ref.[8].

2. For a given concrete strain in the extreme compression fiber ε_{cm} and neutral axis depth *kd* the analysis is performed as follows:

a) The steel strains (ε_{s1}, ε_{s2}, ε_{s3}…) can be determined from similar triangles of the strain diagram. For example, for bar *i* at depth d_i the steel strain is:

$$\varepsilon_{si} = \varepsilon_{cm}\left(\frac{kd - di}{kd}\right) \quad \cdots\cdots\cdots\cdots\cdots\cdots \quad (9)$$

The steel stresses (f_{s1}, f_{s2}, f_{s3} …) corresponding to strains (ε_{s1}, ε_{s2}, ε_{s3}…) may be found from the stress-strain curve for the steel using equations (3). Then the steel forces (S_{s1}, S_{s2}, S_{s3}…) may be found from the steel stresses and the areas of steel, Fig.(4). For example for bar *i* the force equation is:

$$S_i = f_{si} \cdot A_{si} \quad \cdots\cdots\cdots\cdots\cdots\cdots \quad (10)$$

b) The concrete compressive force C_c is made up of two parts, a confined part coming from the core concrete confined by the ties, and the unconfined part coming from the cover concrete. Each part is analyzed separately and both are added to make up the total concrete compressive force, Fig.(5).

3. The force equilibrium equation is:

$$P = C_c + \sum_{i=1}^{n} f_{si}\ A_{si} \quad \cdots\cdots\cdots\cdots\cdots\cdots\cdots\cdots \quad (11)$$

and the moment equilibrium equation:

$$M = C_c\left(\frac{h}{2} - X_c\right) + \sum_{i=1}^{n} f_{si}\ A_{si}\left(\frac{h}{2} - d_i\right) - P\frac{h}{2} \quad \cdots\cdots\cdots \quad (12)$$

Where:

X_c=the moment arm of concrete compressive force (C_c).

The curvature is given by

$$\phi = \frac{\varepsilon_{cm}}{kd} \qquad \text{(13)}$$

4. The method of establishing these relations is based on equilibrium of internal and external forces assuming a linear distribution of strain across the depth of section. Concrete spalling outside the ties has no contribution in internal force calculation at strains more than the maximum unconfined value of (0.004). The moment-curvature curve exhibits a discontinuity at first yield of tension steel and has been terminated when external fiber compressive concrete strain ε_{cm} reaches the maximum compressive strain ε_{cu}, Fig.(4).

Figure (6) shows a comparison between experimental results and the present study results. It is obvious that there is a good agreement between the analytical model and the test results.

Effect of Parameters on Curvature Ductility

The reinforced concrete column shown in Figure (6)[8] is analyzed and the results presented in Figs. (7-11). Each Figure depicts five curves of the moment-curvature relationship. The effects of yield strength for main reinforcement, yield strength of transverse reinforcement, compressive strength of concrete, spacing of ties and axial load on the curvature ductility are

studied with different rate of straining i.e, 0.0001/sec (a typical quasi-static value), 0.001/sec,0.01/sec and 0.1/sec.

Table (2) summarizes the results of the curvature ductility for different parameters (f_y, f_{yt}, f_c',S and axial load). The effects of the above parameters on μ_ϕ for reinforced concrete column sections are as follows:

1. For any strain rate, μ_ϕ increases as f_y decreases. Fig.(12-a) shows that for a (70 MPa) decrease in f_y the increase in μ_ϕ varies in the range of (6%-7%) for all strain rates except for the strain rate of (0.1/sec) for which the change will be about (20%).
2. μ_ϕ increases slightly as f_{yt} increases. Fig. (12-b) shows that for a (70MPa) increase in f_{yt}, there is insignificant increasing in μ_ϕ of (2%) for any strain rate.
3. μ_ϕ increases as f_c' decreases, Fig. (12-c). For instance for a reduction of (3.45 MPa) in f_c' the curvature ductility increases by (17%) and by (7%) for the strain rates of (0.0001/sec) and (0.1/sec) respectively.
4. μ_ϕ is significantly increased when decreasing the axial load, Fig. (12-d). For instance decreasing the axial load from (0.9 $f_c'A_g$) to (0.1 $f_c'A_g$) the curvature ductility ratio increases by about (105%) and (140%) for the strain rates of (0.0001/sec) and (0.1/sec) respectively.
5. It is intuitive to observe the increasing in μ_ϕ with decreasing in spacing of ties, Fig.(12-e). For instance

reducing the spacing from (125 mm) to (50 mm) increases the curvature ductility ratio by (24%) and by (12%) for the strain rates of (0.0001/sec) and (0.1/sec) respectively.

Effects of Strain Rate

Any increase in the rate of loading usually increases both the compressive strength of concrete and the yield strength of steel, Figs.(2,3). Hence it may be expected that the moment capacity of reinforced concrete columns increases with increasing in the loading rate.

Figures (7-11) present the moment-curvature relationships derived analytically under different rates of loading. These rates are 0.0001/sec (a typical quasi-static value), 0.001/sec, 0.01/sec (typically expected under seismic loads) and 0.1/sec (a typical value under impulsive loads) [1].

Table (2) and Fig.(12) show the effect of strain rate on the curvature ductility for different parameters, these effect are :

1. For different yield strength of the main reinforcement the curvature ductility factor under the strain rate of (0.1/sec) increased an average by about (80%) over the curvature ductility under static load, Fig.(12-a).
2. For different yield strengths of the transverse reinforcement the curvature ductility factor under the strain rate of (0.1/sec) increased an average by about (50%) as compared to the static loading, Fig.(12-b,e).

3. For different concrete compressive strengths the average increase in curvature ductility under the strain rate of (0.1/sec) is about (35%) compared to the static loading, Fig.(12-c).
4. The average increase in curvature ductility under the axial force in the range of (0.1 $f_c'A_g$) to (0.9 $f_c'A_g$) is about (25%) for the strain rate of (0.1/sec) compared to the static load condition for which the strain rate is (0.0001/sec), Fig.(12-d).

Figs.(7-11) show the effect of strain rate on the moment-curvature relationships of the column section for different analysis parameters. Under an axial load of (0.6 $f_c'A_g$) and for different f_y, f_c', f_{yt} and ties spacing the average increase in moment capacity at strain rate of 0.1/sec over the static rate is (35%), Figs.(7,8,9 and 11). This increment has been found to vary in the range of (20%) to (80%) for the axial loads (0.1 $f_c'A_g$) and (0.9 $f_c'A_g$) respectively, Fig.(10).

CONCLUSIONS

Based on the results obtained in the present study, the following conclusions can be drawn:

1. The curvature ductility factor increases as the concrete compressive strength decreases, the results show that a reduction of (3.45 MPa) in the concrete compressive strength increasing the curvature ductility by (17%) and (7%) for the strain rates of (0.0001/sec) and (0.1/sec) respectively.

2. The curvature ductility factor increases as the steel yield strength decreases, the results show that decreasing (70 MPa) in the steel yield strength will increase the curvature ductility in the range of (6%-7%) for all strain rates except for the strain rate of (0.1/sec) for which the change will be about (20%).
3. The curvature ductility factor slightly increases as the yield strength of the transverse reinforcement increases.
4. The curvature ductility factor is significantly increased as the axial load decreases, the results show that decreasing the axial load from (0.9 $f_c'A_g$) to (0.1 $f_c'A_g$) the curvature ductility ratio increases by about (105%) and (140%) for the strain rates of (0.0001/sec) and (0.1/sec) respectively.
5. The curvature ductility factor increased by (80%) under the strain rate of (0.1/sec) over the static strain rate for different yield strengths of the main reinforcement.
6. The curvature ductility factor increased by (50%) for a strain rate of (0.1/sec) as compared to the static loading for different yield strengths of the transverse reinforcement.
7. The average increase in curvature ductility under the axial force is about (25%) for the strain rate of (0.1/sec) as compared to the static load condition.

REFERENCES

1. Soroushian, P. and Sim, J. "Axial Behavior of R.C. Columns Under Dynamic loads" ACI Jor. November – December 1986, pp 1018 - 1025.
2. Al Haddad, M. S. "Curvature Ductility of R.C. Beams Under Low & High Strain Rates" ACI Structural Jor. , Vol. 92, No. 5, Sep. – Oct. 1995, pp 526 – 534.
3. Razvi,S. & Saatciaglu ,M. "Confinement Model for High Strength Concrete " Jor. Str. Eng. ASCE, March, 1999.
4. Park ,R. ,Priestley, M. J. N. and Gill, W. D. "Ductility of Square Confined Concrete Columns" ASCE Vol. 108 ,No. St4, April, 1982, pp 929 – 950.
5. Soroushian, P. "Steel Mechanical Properties at Different Strain Rates" ASCE Jor. Str. Eng., Vol. 113, No. 4, April, 1987, pp. 663 – 672.
6. Li Bing, Park, R. and Tanka, H., “Stress-Strain Behavior of High Strength Concrete Confined by Ultra High and Normal Strength Transverse Reinforcements” ACI Str. Jor. May-June, 2001.
7. Park and Paulay “Reinforced Concrete Structures” 1975.
8. Sakai, K. and Sheikh, S. A. "What do we know about Confinement in R.C. Columns? A Critical Review of Previous Work and Code Provisions "ACI Str. Jor. Vol. 86, No. 2, Mar. – Apr., 1989, pp. 192 – 207.

Table (1) Dynamic to Static Ratios of the Yield and Ultimate Stresses of Steel and its Strain Hardening and Ultimate Strains

	Strain-Rate (έ) 1/sec					
	10^{-5}	10^{-4}	10^{-3}	10^{-2}	10^{-1}	1
f_y =307 MPa						
f_y '/ f_y	0.92	1.23	1.29	1.34	1.39	1.44
f_u '/ f_u	0.92	0.96	0.99	1.04	1.08	1.12
$\varepsilon_h'/\varepsilon_h$	0.99	1.31	1.63	1.95	2.27	2.59
$\varepsilon_u'/\varepsilon_u$	0.99	0.99	0.99	0.99	0.99	1.00
f_y =345 MPa						
f_y '/ f_y	1.20	1.25	1.29	1.34	1.39	1.44
f_u '/ f_u	0.92	0.96	0.99	1.04	1.07	1.11
$\varepsilon_h'/\varepsilon_h$	0.99	1.26	1.54	1.81	2.08	2.35
$\varepsilon_u'/\varepsilon_u$	0.99	0.98	0.97	0.97	0.96	0.95
f_y =414 MPa						
f_y '/ f_y	1.25	1.28	1.32	1.36	1.39	1.43
f_u '/ f_u	0.93	0.96	0.99	1.03	1.07	1.10
$\varepsilon_h'/\varepsilon_h$	0.99	1.18	1.37	1.56	1.74	1.93
$\varepsilon_u'/\varepsilon_u$	0.99	0.96	0.94	0.91	0.89	0.86

Table (2) Curvature Ductility μ_{ϕ} for Different Strain Rates

Strain-Rate (έ) 1/sec					*Static*
f_y *(MPa)*	*0.0001*	*0.001*	*0.01*	*0.1*	
414	3.75	4.37	5.23	5.76	3.49
345	4.17	4.92	5.32	6.55	3.51
276	4.23	5.01	6.13	7.71	3.95
f_{yt} *(MPa)*					
414	4.15	4.40	5.27	5.79	3.95
345	3.86	4.31	5.16	5.68	3.85
276	3.57	4.16	5.04	5.54	3.48
f_c' *(MPa)*					
17.24	6.78	6.98	7.33	7.61	6.63
20.7	6.07	6.47	6.79	7.11	5.93
24.14	4.98	5.51	6.14	6.68	4.64
27.6	4.22	4.96	5.59	6.27	3.93
P/ f_c' Ag					
0.1	20.93	22.35	23.20	24.38	19.53
0.3	10.26	11.79	11.81	11.94	10.07
0.5	6.38	7.17	7.79	7.81	6.17
0.7	3.10	3.53	3.74	4.13	2.93
0.9	0.93	0.94	0.96	0.99	0.91
S(mm)					
50	5.83	6.31	6.98	7.35	5.69
75	4.72	5.45	5.98	6.77	4.67
100	4.06	4.62	5.41	5.89	4.03
125	3.02	3.78	4.59	5.20	2.93

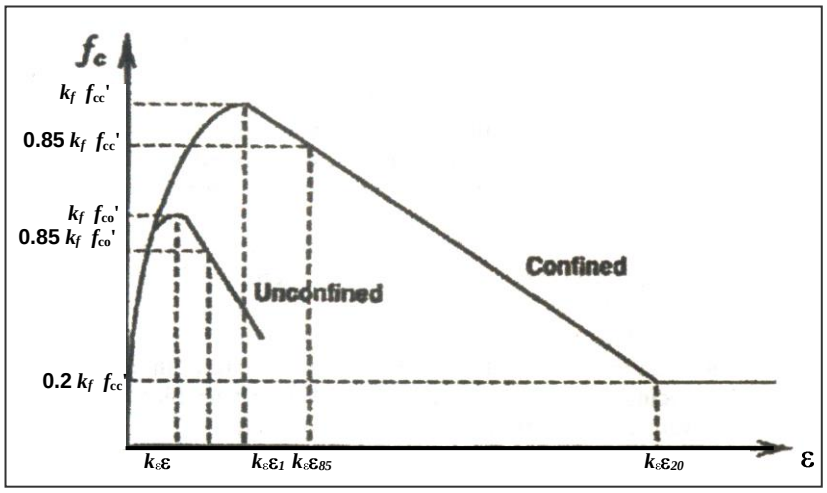

Figure (1) Strain rate modified stress-strain relationship for concrete[1]

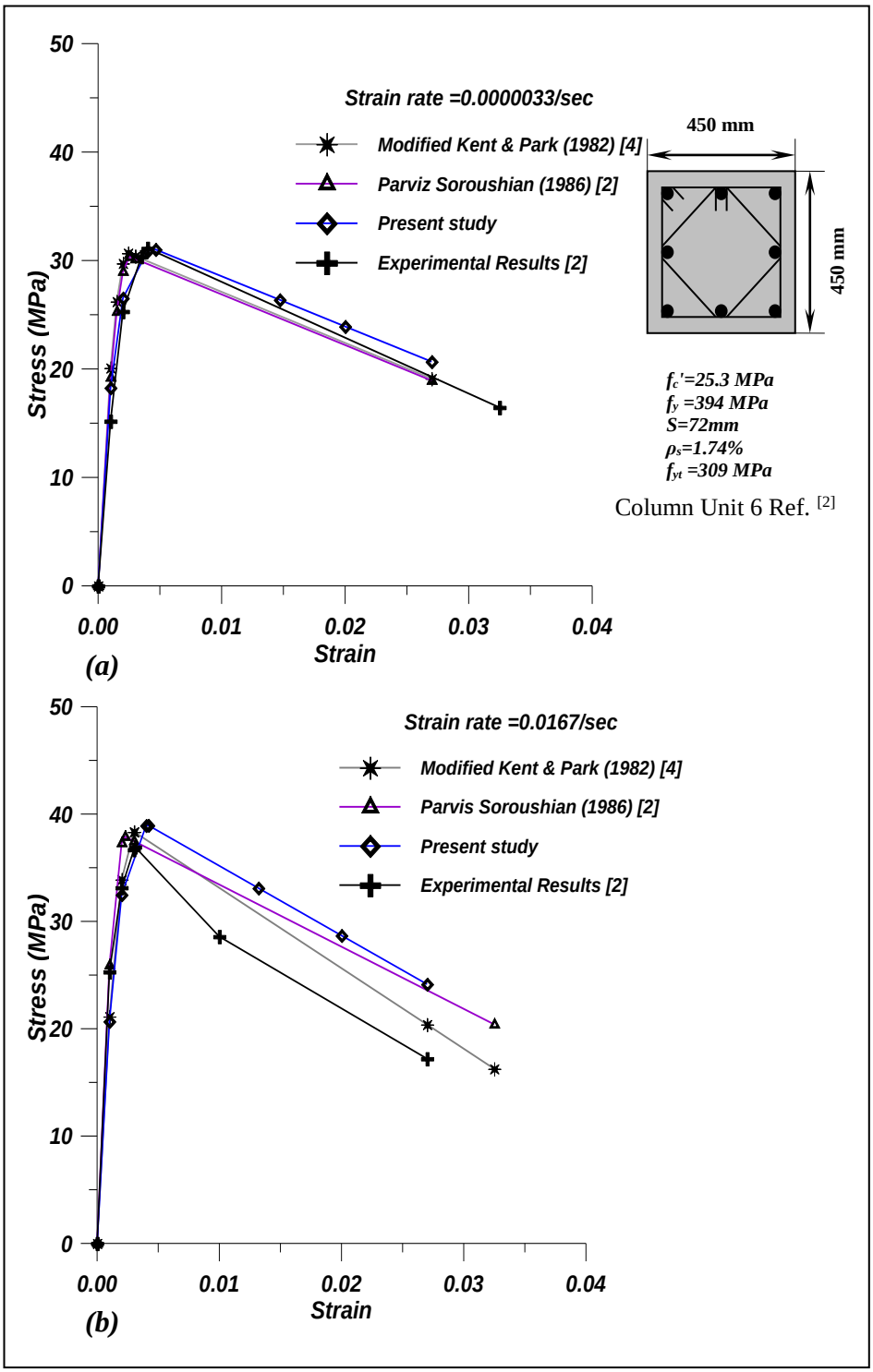

Figure (2) Comparison among the Constitutive Models for Concrete with Test Results (a) Low strain rate of 0.0000033/sec (b) High strain rate of 0.0167/sec

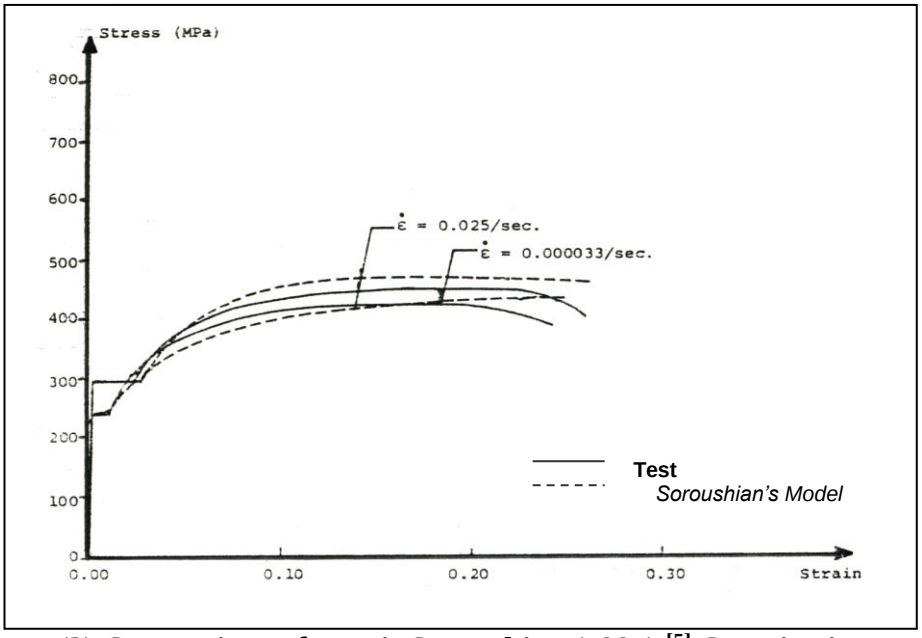

Figure (3) Comparison of Parvis Soroushian (1987) [5] Constitutive Model of Steel with Test Results for f_y=235 MPa

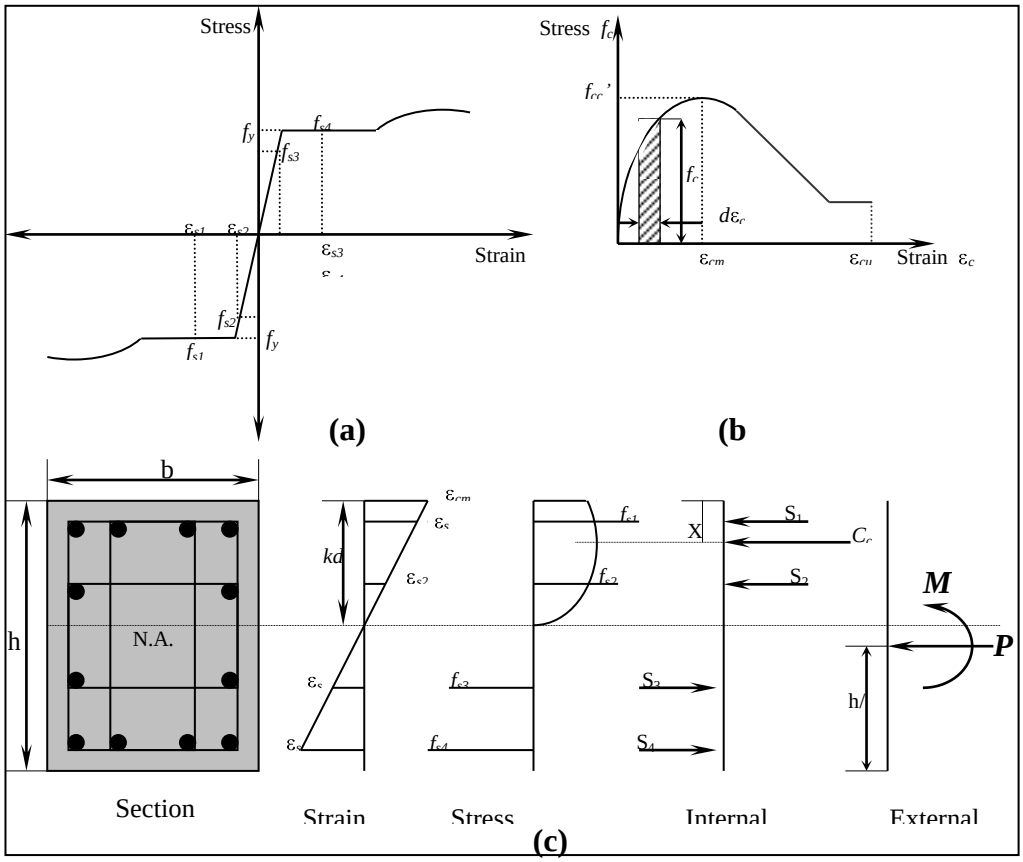

Figure (4) Theoretical Moment Curvature Analysis (a) Steel in tension and compression.

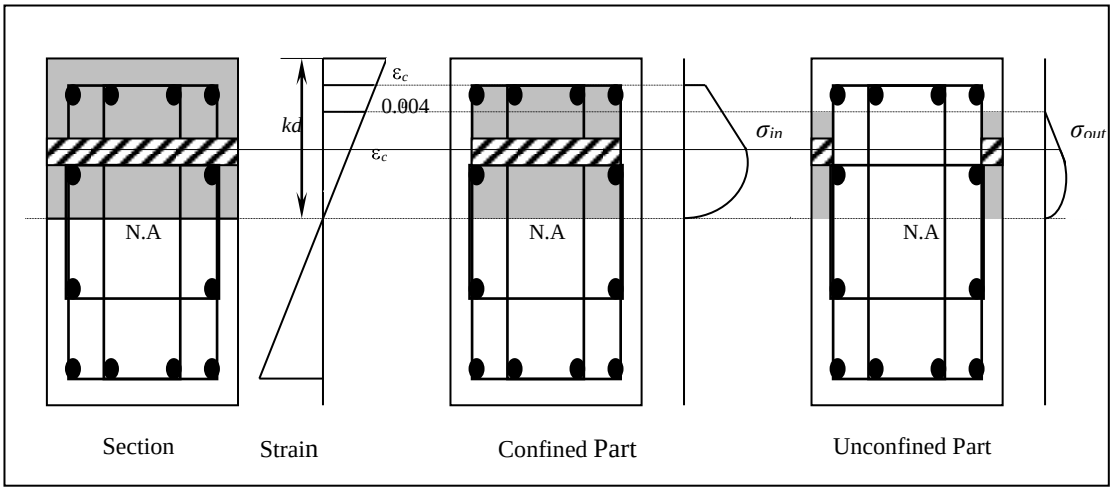

Figure (5) Concrete Section Analysis.

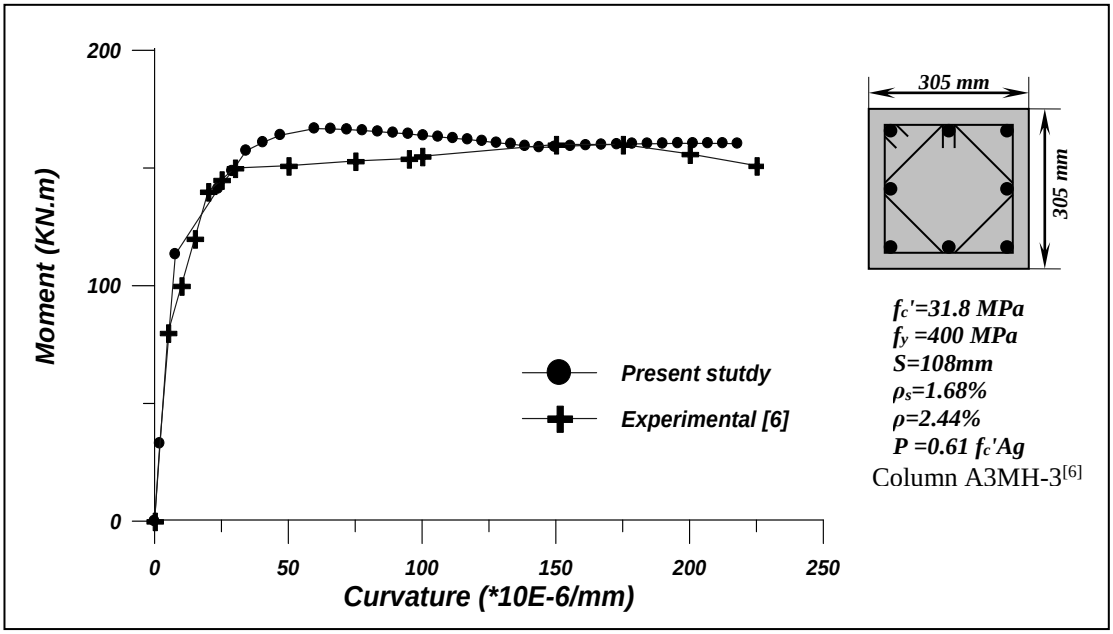

Figure (6) Comparison between Experimental Results and the Present Study Results [6]

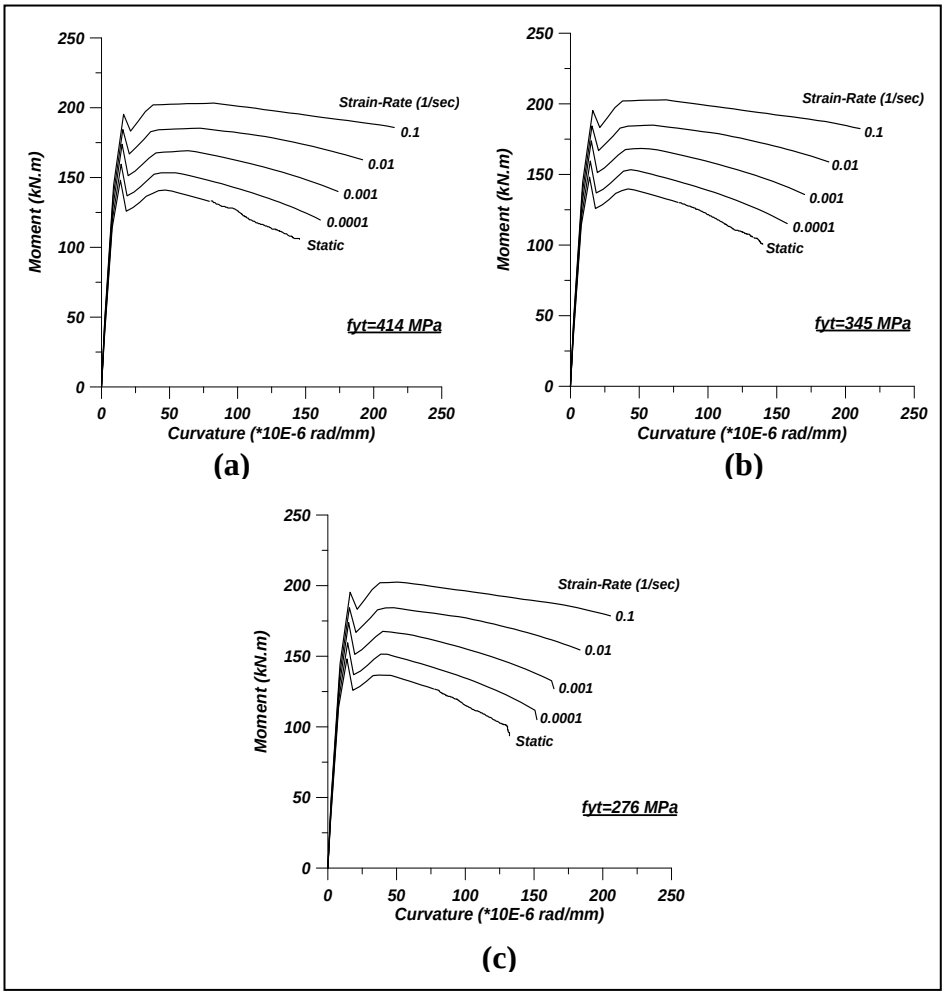

Figure (8) Effect of Strain-Rate on the Moment Curvature Relationship for Different Yield Strength of Transverse Reinforcement f_c'=31.8 MPa , f_y =400 MPa , P=0.6 $f_c'A_g$

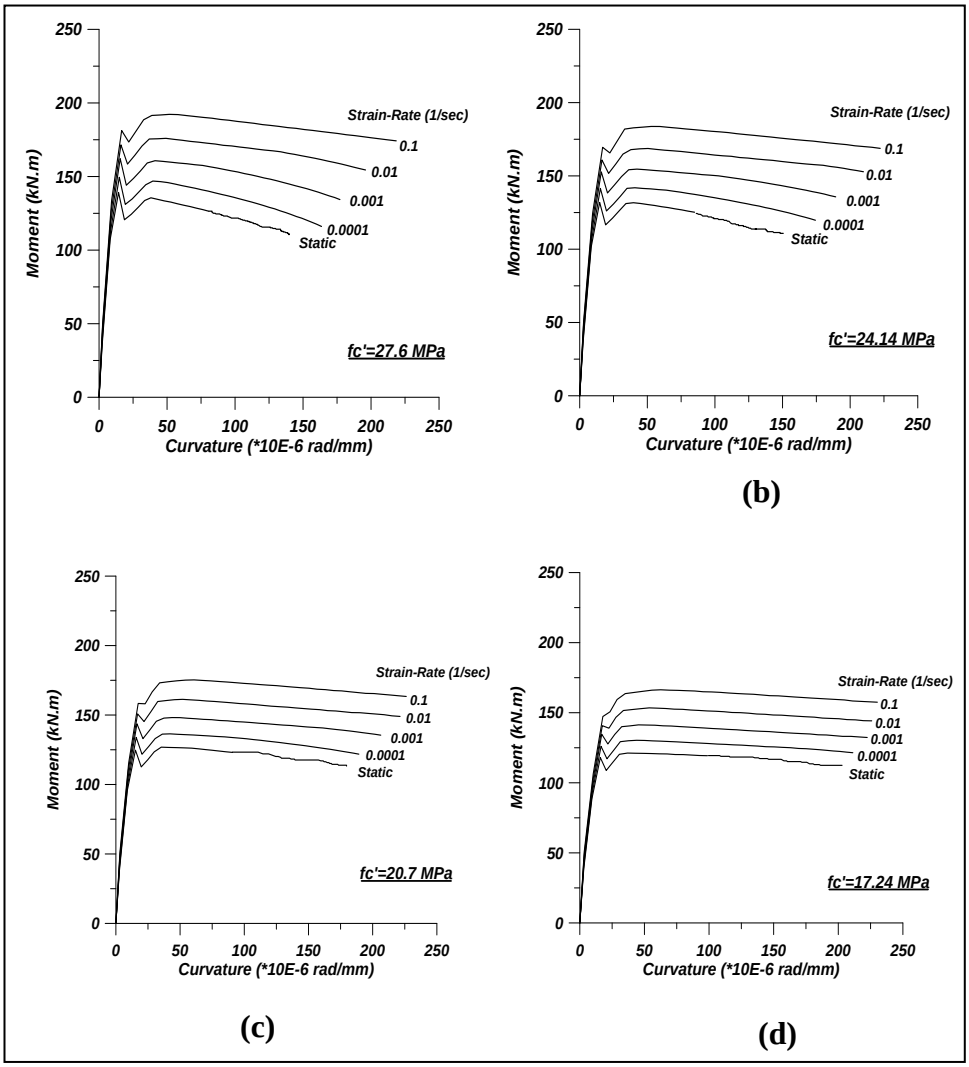

Figure (9) Effect of Strain-Rate on the Moment Curvature Relationship for Different Compressive Strength of Concrete f_y =400 MPa, f_{yt} =276 MPa ,P=0.6

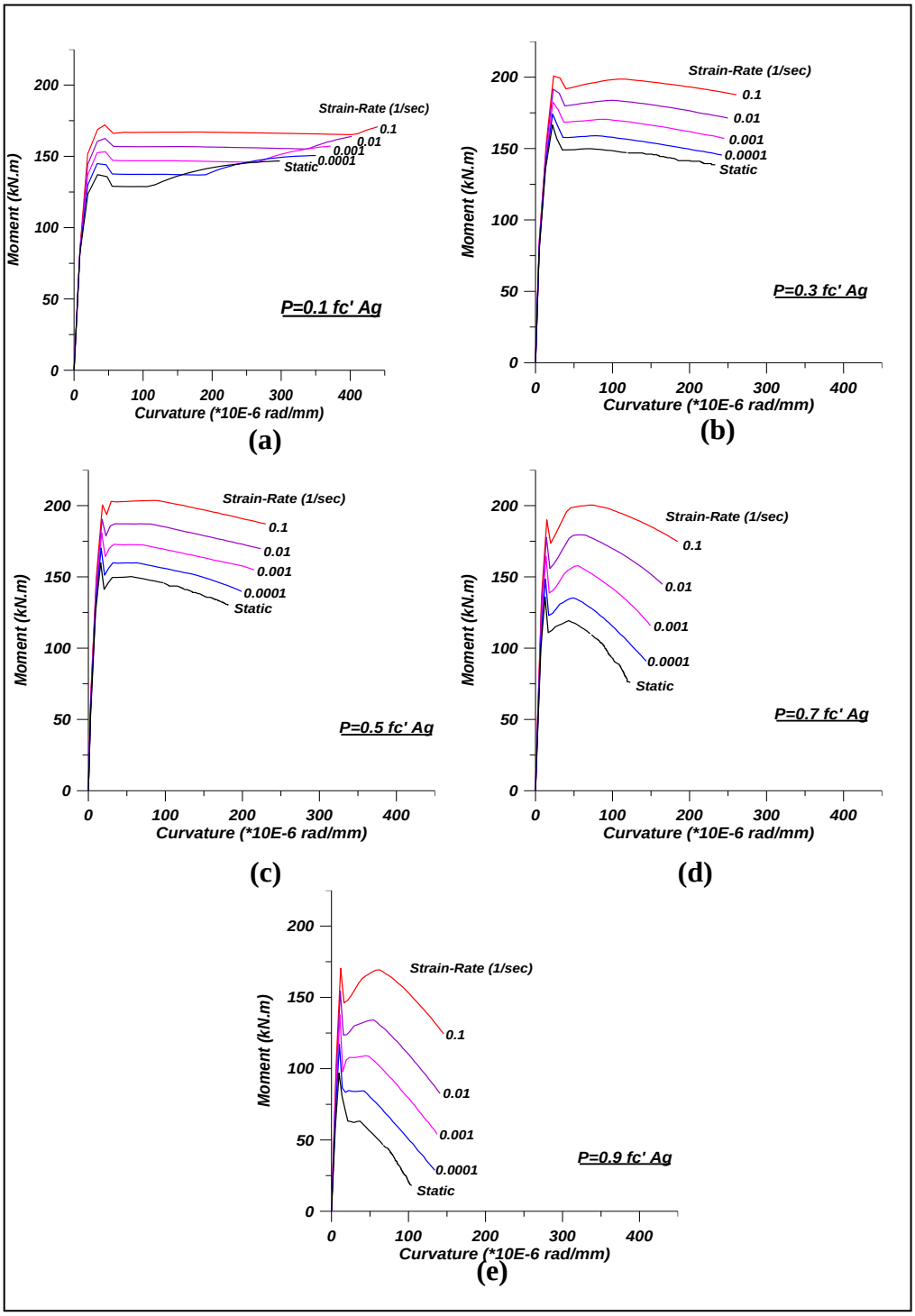

Figure (10) Effect of Strain-Rate on the Moment Curvature Relationship for Different Axial Load f_c'=31.8 MPa , f_y =400 MPa , f_{yt} =276 MPa

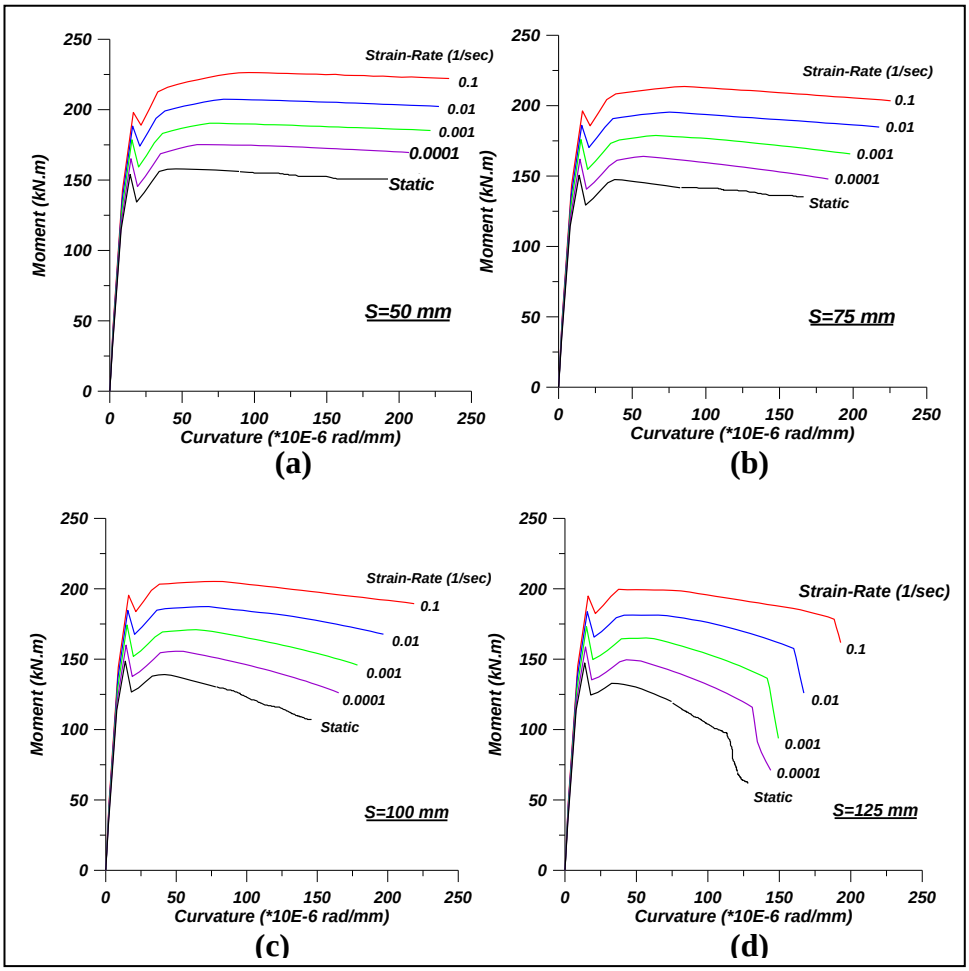

Figure (11) Effect of Strain-Rate on the Moment Curvature Relationship for Different Spacing of Transverse Reinforcement f_c'=31.8 MPa, f_y =400 MPa ,

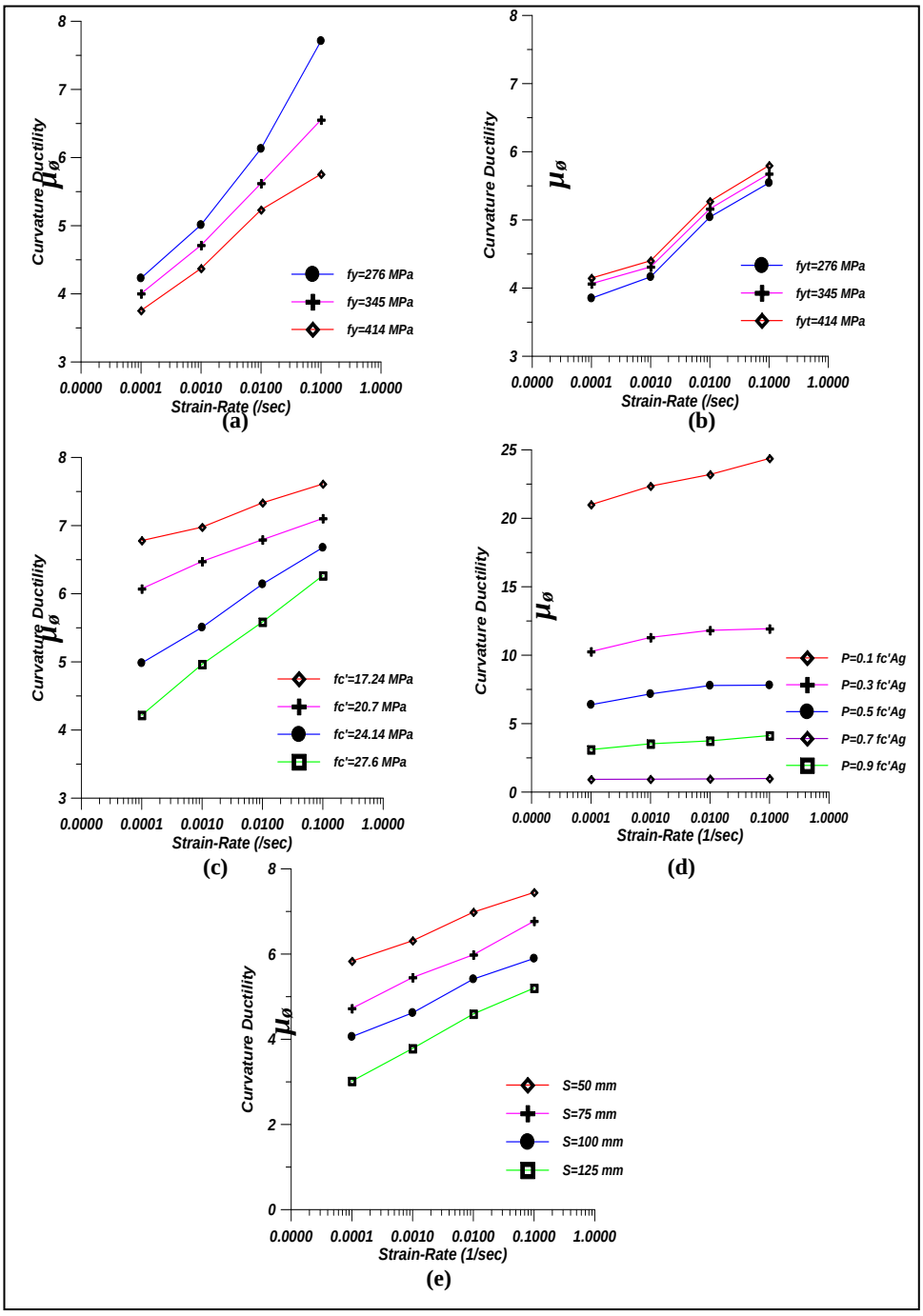

Figure (12) Effect of strain rate on curvature ductility for different:
(a) Effect of steel yield strength for main reinforcement (f_c'=31.8 MPa, f_{yt} =276 MPa, P=0.6 f_c'A_g,S=108mm)
(b) Effect of steel yield strength for transverse reinforcement (f_c'=31.8 MPa, f_y=400 MPa, P=0.6f_c'A_g, S=108mm)
(c) Effect of concrete compressive strength (f_y =400 MPa, f_{yt} =276 MPa, P=0.6 f_c'A_g, S=108mm)
(d- Effect of axial load (f_c'=31.8 MPa, f_y =400 MPa, f_{yt} =276 MPa, S=108mm)
(e) Effect of spacing of ties (f_c'=31.8 MPa , f_y =400 MPa , f_{yt} =276 MPa , P=0.6 f_c'A_g)

مطيلية التقوس لمقاطع الأعمدة الخرسانية المسلحة تحت تأثير نسب قيم زمنية مختلفة للانفعال

د. ثامر خضير العزاوي د. رعد كريم العزاوي تغريد حسن إبراهيم

أستاذ مدرس مهندس

قسم الهندسة المدنية

كلية الهندسة– جامعة بغداد

الخلاصة

قدم هذا البحث دراسة نظريه لقابلية مطيلية التقوس لمقاطع الأعمدة الخرسانية المسلحة. تم في هذه الدراسة الأخذ بنظر الاعتبار تصرف كل من الخرسانة وفولاذ التسليح تحت تأثير نسب قيم زمنية مختلفة للانفعال. لحساب مطيلية التقوس تم كتابة برنامج كومبيوتر واخذ بنظر الاعتبار الانفصال الحاصل في غطاء الكونكريت. لقد تم استعمال مخططات متحسسة للمعدل الزمني للانفعال لكل من الفولاذ والخرسانة وذلك لتوقع علاقة العزم مع التقوس لمقاطع الأعمدة. المتغيرات التي استخدمت في هذه الدراسة هي مقاومة الخضوع لفولاذ التسليح الرئيسي، مقاومة الخضوع لفولاذ التسليح الثانوي، مقاومة الانضغاط للكونكريت، مسافات روابط الأعمدة، و القوة المحورية. النتائج المستحصلة من الدراسة أشارت إلى أن زيادة المعدلات الزمنية للانفعال تحسن من المقاومة و قابلية العزم لمقاطع أعمدة الكونكريت المسلح.

الكلمات الدالة

مطيلية التقوس، الأعمدة، الخرسانة المسلحة، المعدل الزمني للانفعال.